Coupled adhesion of bacteria to surfaces

Skogvold, Rebecca van der Westen

CHAPTER 5

Bacterial Adhesion and Detachment to Oscillating Hydrophobic and Hydrophilic Surfaces Studied in a Quartz Crystal Microbalance

Rebecca van der Westen, Aldona Mzyk, Jelmer Sjollema, Prashant K. Sharma, Henny C. van der Mei and Henk J. Busscher

ABSTRACT

Variation of the driving voltage and crystal oscillation amplitude in quartz crystal microbalance with dissipation (QCM-D) has seldom been explored but offers interesting possibilities to measure (bio)colloidal particle adhesion forces and characteristics of the bond, as achieved during different development histories. To this end, we built a modified QCM, referred to as a vector network analyzer (VNA) which allows to vary the QCM driving voltages from 0.01 V to 0.4 V. Quality factors Q of the VNA-based QCM, using the same crystals and chamber as the Q-sense, were found comparable with those of the Q-sense QCM-D and were used to calculate the oscillation forces exerted on the (bio)colloidal particles during adhesion to an oscillating crystal. Forces to prevent (bio)colloidal particle adhesion ranged from 0.2 pN to 30 pN, while forces required to detach adhering particles were higher and ranged from 2 pN to 30 pN. Although these forces are orders of magnitude smaller than generally derived from atomic force microscopy (AFM), they are of the same order of magnitude as obtained using optical tweezers and flow displacement systems. This negates often voiced criticism on QCM data that its high oscillation frequency influences (bio)colloidal particle adhesion. However, bond characteristics, derived in a coupled resonator model based on the routine QCM output and use of a phenomenological Kelvin-Voigt model, varied with the oscillation forces applied during adhesion.

SIGNIFICANCE

Bacterial adhesion forces to surfaces are hard to measure and values differing orders of magnitude linger through current literature. This work adds a simple, and easy to interpret instrument to measure (bio)colloidal adhesion forces, that coincide generally well with force values obtained using optical tweezers and flow displacement systems, but not with forces obtained using AFM. Importantly, the high frequency oscillations in QCM appear not to influence the adhesion forces to the extent that make them incomparable with forces obtained under unidirectional fluid shear forces. Therewith, this work yields a significant additional method to measure bacterial and colloidal particle adhesion forces. Moreover, it helps solve the question whether bacterial adhesion forces are in the nN-range (AFM) or pN- range (QCM, optical tweezers and flow displacement systems).

INTRODUCTION

Employing resonator-based sensing platforms to determine molecular adsorption and (bio)colloidal particle adhesion in biological systems has been widely used in the last 50 years, most notably making use of the quartz crystal microbalance with dissipation (QCM-D). In QCM-D, changes in resonance frequency of oscillating crystals due to molecular adsorption or (bio)colloidal adhesion are registered, along with the characteristic damping of the crystal's oscillation upon arresting its amplitude drive (dissipation). In a first approximation,[1] adsorbed masses (Δm) are related to a change in frequency (Δf) and overtone number (n) according to[2]

$$\Delta m = (C/n)\Delta f \quad [1]$$

in which

$$C = \frac{t_q \rho_q}{f_0} \quad [2]$$

in which C is the sensitivity constant for the crystal at its fundamental frequency (f_0), t_q is the thickness of the quartz crystal disc, and ρ_q the density of the crystal. Note that in case of adsorption, (Δf) should be negative.

The linear relation presented by Eq. 1 can be violated due to structuring of interfacial water on the crystal surface, water entrapment in between adsorbed molecules or adhering (bio)colloidal particles, and viscoelasticity of the bond, all leading to damping of the crystals oscillation, that can either be expressed in terms of the changes in dissipation (ΔD) given by

$$\Delta D = \frac{1}{\pi f \tau} \quad [3]$$

in which f is given by $f = f_0 - f_R$, where f_0 is the resonance frequency and f_R a reference frequency filtered with a low pass band filter, and τ is the decay time. Dissipation is related to the half band half width (Γ) of the sensor resonance frequency according

$$\Gamma = \frac{D f_S}{2} \quad [4]$$

in which f_s is the sensor resonance frequency. With respect to (bio)colloidal particle adhesion, Eq. 1 loses its validity, as particles have been demonstrated to form a coupled resonator system with the

oscillating crystal, giving rise to positive frequency shifts and a frequency of zero crossing to negative frequency shifts, indicating a match of the sensor and particle resonance frequencies.[3]

Adhesion and detachment of (bio)colloidal particles to the oscillating crystal surface can be controlled by changing the oscillation amplitude within a QCM instrument.[2,4,5] The amplitude of the crystal's oscillation (A) scales linearly with the driving voltage (V_d) applied over the crystal (see Figure 1), according to

$$A = 1.4\ Q\ V_d \qquad [5]$$

in which Q is the crystal's quality factor, defined as

$$Q = f_0/(2\Gamma) \qquad [6]$$

Q reportedly ranges from 2500 to 5000 in aqueous systems at lower overtones.[2]

Although driving voltages are seldom reported in QCM studies, driving voltages can be adjusted. In the Q-sense instrument, driving voltages can be adjusted in ten incremental steps, ranging from 0.2 to 10, albeit resulting driving amplitudes are given in arbitrary units and difficult to calculate in absolute units due to absence of the necessary data. In its standard mode, the driving voltage of the Q-sense is adjusted automatically to yield an optimal output. Variation of the driving voltage is accompanied by a small change in resonance frequency of the crystal, ascribed to piezoelectric stiffening of the crystal and not due to possible (minor) temperature increases. Moreover, changes in resonance frequency upon changing oscillation amplitudes are confined to 100 – 200 Hz and therewith orders of magnitude smaller than the common crystal resonance frequencies, both in air as well as in aqueous solutions.[6]

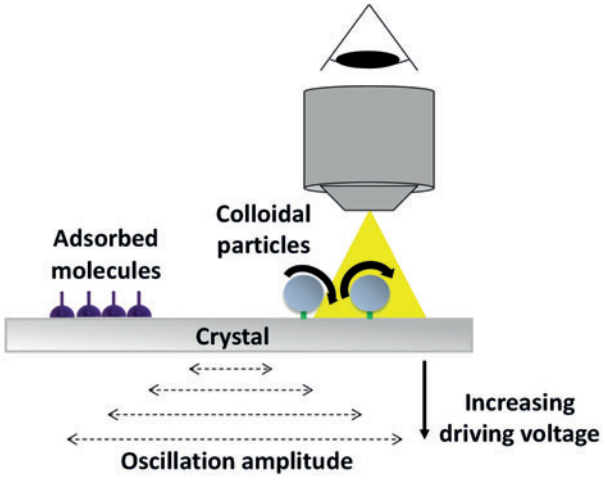

Figure 1. Driving voltages relate with the crystal's oscillation amplitudes according to Eq. 5 and cause an oscillation force on adsorbed molecules (Eq. 7) and adhering (bio)colloidal particles (Eq. 8).

The influence of driving voltage on the QCM output depends on the system studied through the quality factor (Q) in Eq. 6. Adsorption of streptavidin to a biotinylated stationary or oscillating crystal was essentially the same.[2] This demonstrates that the streptavidin-biotin bond is stronger than the oscillation force exerted on a bound molecular mass, as given by

$$F_{osc-M} = \frac{2}{7} m A_{osc} (2\pi f_0)^2 \qquad [7]$$

in which $F_{osc\text{-}M}$ is the oscillation force acting on a molecular mass (m) adsorbed to an oscillating crystal sensor with oscillation amplitude (A_{osc}).[5,7] On the other hand, adhesion of 200 nm polystyrene particles coated with a streptavidin analogue to biotinylated, oscillating crystal surfaces reduced to less than 20% upon increasing the driving voltage from 0 to 10 V.[2] However, detachment of such particles adhering to a stationary crystal could not be established upon oscillating the crystal. This confirms that forces required to prevent (bio)colloidal particle adhesion are smaller than the forces required to detach already adhering particles. The exact force values at which (bio)colloidal particle adhesion can be prevented or detachment can be stimulated greatly depend on the method applied. For instance, atomic force microscopy,[8] use of optical tweezers[9] and flow displacement systems[10,11] have consistently given highly different values for bacterial adhesion forces that range from the nN to the pN range.

The oscillation force exerted on adhering (bio)colloidal particles ($F_{osc\text{-}P}$) by an oscillating QCM crystal increases with the particle radius and assuming particle vibration around its vertex (see Figure 2), can be calculated to be

$$F_{osc-P} = \frac{16\rho R^3 (CQV_d)^2 f_0^2}{5\sqrt{(CQV_d)^2 + 4R^2}} \quad [8]$$

in which ρ is the density of the (bio)colloid, R the particle radius, and C is an experimental constant (1.4 x 10^{-12} m/V).[12]

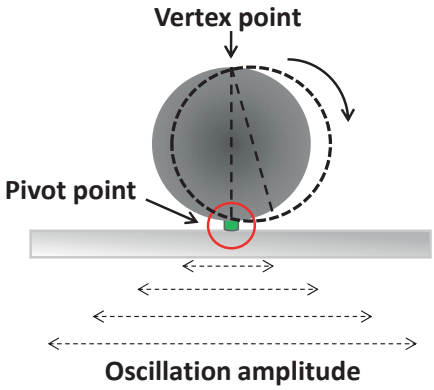

Figure 2. Schematic representation of the rotation and wiggling of a (bio)colloidal particle adhering to an oscillating crystal around its vertex point. Adapted from Yuan et al.[6]

Varying of the driving voltage in QCM and monitoring the detachment and adhesion of colloidal particles in antibody-antigen complexes has been suggested as a tool in biomedical diagnostics,[5] but may thus also offer ample opportunities to study bacterial adhesion mechanisms to surfaces. Bacterial adhesion to a surface has been described in a Kelvin-Voigt model as a viscoelastic bond, modeled by a spring in parallel with a dashpot. Higher spring constants were obtained using QCM for a bald streptococcal strain than for a strain with fibrillar surface tethers, and drag coefficients increased for the bald streptococcus with the ratio of electron-donating over electron-accepting parameters of the crystal surface free energy,[13] while for the fibrillated strain the drag coefficient was similar on all crystal surfaces. This suggests that the drag experienced by resonator-coupled, fibrillated bacteria tethered to a surface, is more influenced by the viscosity of the bulk water than by structuring of interfacial water closely adjacent to the crystal surface. Oppositely, bacteria lacking fibrillar surface tethers were mass-coupled just above the crystal surface and accordingly probed a drag due the thin layer of interfacial water that is differently structured on hydrophobic and hydrophilic surfaces. Detachment of adhering bacteria has not yet been measured as induced by the drag caused by crystal oscillations in QCM. QCM analysis of bacterial adhesion at different oscillation amplitudes may yield new insights into non-linear effects occurring during adhesion and detachment, such as strain

stiffening or weakening of surface tethers with a potential impact in coupled-resonator models,[14] describing an analytical relationship between the observed frequency and dissipation shifts with spring constants, drag coefficients and particle masses.

This chapter aims to explore the possibilities in varying the crystal oscillations in QCM with respect to increasing our understanding of bacterial adhesion and detachment to and from surfaces. The specific aims of this chapter are:

1. Comparison of the quality factor, Q, of the Q-sense QCM-D as applied in previous chapters and a new, home-built QCM-based vector network analyzer (VNA). Since the control offered by the Q-sense QCM-D over the driving voltage controlling the crystal oscillations is not trivial, a VNA-based QCM was constructed offering full control over the driving voltage and resulting oscillation amplitude. Considering the use of the Q-sense instrument in previous chapters, a formal comparison was thought necessary.

2. Comparison of the detachment of adhering streptococci with and without fibrillar surface tethers, and of polystyrene particles of similar size from a hydrophobic and hydrophilic crystal surface, as induced by an oscillating crystal in an aqueous phase. Oscillation forces will be varied by increasing the driving voltage after adhesion to derive a detachment force. Detachment forces obtained will be compared with bacterial detachment forces for the two strains as reported in the literature using different methods.

3. Comparison of streptococcal and polystyrene particle adhesion to hydrophobic and hydrophilic crystal surfaces in presence of crystal oscillation during adhesion to derive a force required to prevent bacterial adhesion. Forces obtained to prevent bacterial adhesion will be compared with bacterial detachment forces for the two strains as reported in the literature using different methods.

4. The QCM response obtained in selected experiments will be analyzed using a phenomenological Kelvin-Voigt resonator model in order to see whether the resulting spring constants, drag coefficients and particle masses depend on the oscillation forces applied during adhesion and relate with the different structuring of water above a hydrophobic or hydrophilic crystal surface.

EXPERIMENTAL SECTION

The VNA-based QCM. The VNA spans a 0.05-60 MHz frequency range, hence up to 6 frequency overtones (5, 15, 25, 35, 45, and 55 MHz) can be measured. To explore the driving voltage dependence of the resonances, the output of the VNA was connected to an RF Power Amplifier (ZHZ-1-2W-S+; Mini Circuits, Brooklyn, NY, US) through a digital step attenuator (ZX76-31R5-SP-S, Mini Circuits, Brooklyn, NY, US), allowing the driving voltage to be varied from 0.01 V to 0.4 V. The quartz crystal was mounted in a window-equipped chamber (Model Q-sense E1, Q-sense, Gothenburg, Sweden) and coupled to

the output of RF Power Amplifier using a Wheatstone bridge (Figure 3). The window chamber itself containing the sensor crystal was mounted underneath a microscope (Leica DM2500 M, Rijswijk, The Netherlands) equipped with a CCD camera (Model A101, Basler vision technologies, Ahrensburg, Germany) for monitoring the number of adhering (bio)colloidal particles on the crystal surface.

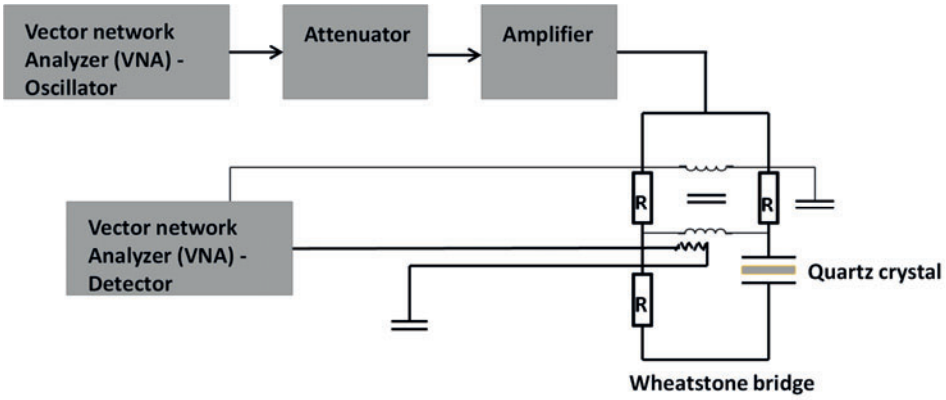

Figure 3. Schematics of the VNA-based QCM.

The Q-sense QCM-D. The QCM-D spans a 1-70 MHz frequency range, hence up to 7 frequency overtones (5, 15, 25, 35, 45, 55, and 65 MHz) can be measured. The Q-sense QCM-D uses the "ring-down" technique. In ring-down, the resonator is excited by a RF-pulse, where the frequency is about the same as the expected resonance frequency. Following that, the excitation is shut off and the oscillation is allowed to decay. The decay time is equal to $1/(2\pi\Gamma)$.[15] All Q-sense QCM-D experiments were carried out using the same window-equipped chamber, crystals and microscopic observation of particle adhesion, as employed in the experiments with the VNA-based QCM-D.

Preparation of QCM Sensor Surfaces. 14 mm AT-cut gold-coated quartz sensors (Q-sense, Gothenburg, Sweden) were cleaned prior to each experiment by immersing in a 3:1:1 mixture of ultrapure water (specific resistance > 18 MΩ cm), ammonia (NH_3) (Merck, Darmstadt, Germany) and hydrogen peroxide (H_2O_2) (Merck, Darmstadt, Germany) at 70°C for 15 min, followed by 15 min of UV/Ozone treatment. Quartz crystals used, had a resonance frequency (f_0) of 5 MHz, a thickness (t_q) of 0.33 mm and a density (ρ_q) of 2.65 g/cm^3, yielding a sensitivity constant (C) of 17.3 ng Hz^{-1} cm^{-2} (see also Eq. 2).

In order to coat the QCM crystal sensors with a hydrophobic self-assembled monolayer (SAM), crystals were left immersed in 0.001 M of 1-octadecanethiol (Sigma- Aldrich, Zwijndrecht, the Netherlands) dissolved in 100% ethanol for 18-20 h under mild shaking conditions. To obtain

hydrophilic crystal sensors, crystals were immersed in 0.001 M of 11-mercapto-1-undecanol (Sigma-Aldrich) in 100% ethanol under the above conditions. Contact angles with liquids and resulting surface free energy components and parameters as taken from the literature,[13] of thus prepared crystal surfaces are summarized in Table 1.

Table 1 Water contact angles, and surface free energy components and parameters of QCM crystal surfaces with a hydrophobic or hydrophilic SAM. Data represent averages with standard deviations over three droplets with each liquid on three different crystals.

	Hydrophobic SAM	**Hydrophilic SAM**
Contact angles (degrees)		
Water	94 ± 7	11 ± 1
formamide	20 ± 2	0 ± 0
methyleneiodine	44 ± 6	34 ± 6
Surface free energy components and parameters (10^{-3} J m^{-2})		
γ	38 ± 3	57 ± 4
γ^{LW}	38 ± 3	42 ± 3
γ^{AB}	0 ± 0	15 ± 3
γ^{-}	0 ± 0	53 ± 4
γ^{+}	12 ± 1	1 ± 0
γ^{-}/ γ^{+}	0 ± 0	53 ± 10

Q Factor Determination. In order to allow comparison of the Q-sense and VNA-based QCM, the quality factor, Q (see Eq. 6), was determined for each instrument and for hydrophobically and hydrophilically modified crystals. Moreover, using the quality factor Q, oscillation forces on adsorbed masses and adhering (bio)colloidal particles can be calculated for the VNA-based QCM (Eqs. 7 and 8, respectively).

In order to determine the resonance frequency (f_0) and half-band half-width of the resonance peak (Γ) in the VNA-based QCM (see Figure 3) an alternating voltage is applied to the system, which causes the crystal to oscillate. When the driving frequency matches the crystal resonance frequency, this is observed as a steep decrease of the impedance of the QCM crystal as measured in the "Wheatstone bridge"-configuration (see also Figure 3). The impedance decrease represents both a decrease in the resistance of the crystal (real part of the impedance) and a characteristic phase-shift with respect to the driving voltage (the imaginary part of the impedance). The shift in the resonance

frequency and the changes in bandwidth for adhering (bio)colloids accordingly determine both Δf and ΔΓ.[16]

Since the Q-sense QCM-D is based on the "ring-down" technique,[17] an alternative strategy was applied to determine the Q factor. First an alternating current was applied to oscillate the crystal. When the frequency of the current matches the resonance frequency f_0 of the crystal, a resonance peak is obtained and the driving voltage is turned off, leading to decay of the oscillations. Oscillation amplitude decay over time is recorded. From this decay, the dissipation (D) can be derived (see Figure 4). Subsequently, Eq. 4 can be employed to obtain Γ, which is then used in Eq. 6 to calculate the Q factor of the system.

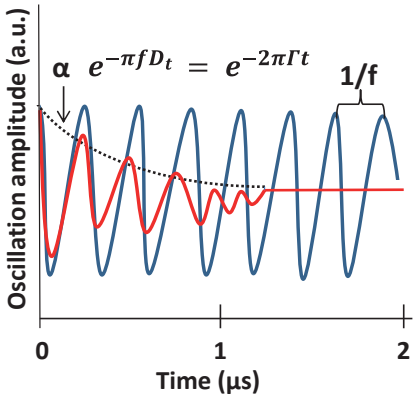

Figure 4. Oscillation amplitude of a QCM-D crystal after "ringing-down" at time zero (putting the driving-voltage to zero) as a function of time. The blue decay curve corresponds to the slower decay of crystal oscillations in air, while the red decay curve relates to decay of crystal oscillations in liquid.

Bacterial Strains, Culture Conditions and Harvesting. *Streptococcus salivarius* HB7 (possessing well-characterized 91 nm fibrils) and HBC12 (devoid of surface appendages)[18] were used in this study. Both *S. salivarius* strains are hydrophilic, and negatively charged under physiological conditions. *S. salivarius* strains were pre-cultured in 10 mL of Todd Hewitt Broth (THB, OXOID, Basingstoke, UK) under static conditions, grown for 24 h at 37°C. After 24 h, pre-cultures were inoculated into 200 mL of THB and maintained under their above conditions for another 16 h. Bacteria were harvested by centrifugation at 5000 g for 5 min at 10°C followed by washing in 100 mL adhesion buffer (50 mM potassium chloride, 2 mM potassium phosphate, 1 mM calcium chloride, pH 6.8). Subsequently, bacteria were sonicated on ice 3 times for 10 s at 30 W (Vibra Cell Model 375; Sonics and Materials Inc., Danbury, CT) to break bacterial chains and obtain single bacteria in suspension. Importantly in order to prevent molecular adsorption in QCM experiments, bacteria were washed once more after sonication to remove any free molecules that might have been released during sonication. Finally,

bacteria were suspended to a concentration of 3 x 10^8 bacteria per mL, as determined by counting in a Bürker-Türk chamber.

Abiotic Particles. Polystyrene particles (Bang Laboratories Inc. Fishers, IN, US), with a diameter of 1 µm similar as streptococci, were selected for this study in order to compare colloidal particle *versus* bacterial adhesion. Prior to experiments, particles were washed twice by centrifugation in 10 mL ultrapure water (specific resistance > 18 MΩ cm), and suspended to a concentration of 2 x 10^8 particles per mL in adhesion buffer.

Detachment Forces of Adhering (Bio)colloidal Particles. In order to determine the oscillation force required to detach adhering streptococci or polystyrene particles in the VNA-based QCM, a (bio)colloidal suspension was perfused through the chamber at a flow rate of 300 µL min^{-1} for 1 h in absence or presence of crystal's oscillations. Subsequently, buffer was perfused to remove non adhering (bio)colloids from the QCM chamber as well as to replace it with buffer. Next, after enumeration of the number of adhering (bio)colloidal particles, a driving voltage was applied (0.01 V, 0.1 V or 0.4 V) to cause crystal oscillation at different oscillation amplitudes and forces for 30 min, during which perfusion with buffer was continued at the same flow rate as during adhesion. Immediately after 30 min detachment, Δf and ΔΓ were measured applying a driving voltages of 0.01 V, 0.1 V or 0.4 V (requiring about 5 min), and adhering particles were enumerated again. Data have been analyzed pairwise within a separate experiment to quantitate numbers of detached (bio)colloids in each experiment, after which numbers of (bio)colloids after detachment were calculated with respect to the average number of adhering (bio)colloids prior to detachments in order to reduce the influence of biological variations within experiments. All data were performed in duplicate.

Forces Required to Prevent Adhesion. In order to determine the force required to prevent (bio)colloidal particle adhesion the window chamber was perfused (flow rate of 300 µL min^{-1}) for 1 h with a (bio)colloidal suspension in buffer during crystal oscillation at different driving voltages (0.01 V, 0.1 V and 0.4 V) to cause crystal oscillation at different oscillation amplitudes and forces, followed by perfusion and replacement of the suspension by buffer as well as enumeration of the number of adhering (bio)colloidal particles, requiring about 5 min. Finally, Δf and ΔΓ were measured applying a driving voltages of 0.01 V, 0.1 V or 0.4 V (requiring about 5 min), and adhering particles were enumerated again. All data were performed in duplicate.

Analysis of QCM Measurements. For the data analysis, frequency shifts (Δf) and band width changes (ΔΓ) as well as the number of adhering (bio)colloidal particles immediately after retrieving (Δf) and (ΔΓ), were used to obtain the spring constant (k) and drag coefficients (ξ) of the bond, and the inertial mass of the particle (m_p) according to a phenomenological Kelvin-Voigt resonator model[13,19,20]

$$\Delta f + \frac{i\Delta D f_s}{2} = \frac{f_F m_p}{\pi Z_q} \cdot N_p \left[\frac{\omega_s^3(\omega_p^2 - \gamma^2) - \omega_s \omega_p^4}{(\omega_s^2 - \omega_p^2)^2 + \omega_s^2 \gamma^2} + i \frac{\omega_s^4 \gamma}{(\omega_s^2 - \omega_p^2)^2 + \omega_s^2 \gamma^2} \right] \quad [9]$$

where f_F is the fundamental resonance frequency of the sensor (5 MHz), ω_p is the angular resonance frequency of the particle, ω_s is the angular resonance frequency of the sensor, both given by $2\pi f_p$ and $2\pi f_s$, respectively. γ equals ξ/m_p. Z_q is the acoustic impedance of the AT-cut quartz crystal (8.8×10^6 kg m^{-2} s^{-1}), and N_p is the number of adhering particles per unit area (m^{-2}). All data derived represent those yielding the smallest root mean square deviation (RMSD) of the fit.

Statistical Analysis. All data are presented as means ± standard deviations. Results were compared pair-wise for the two bacterial strains and polystyrene particle, as well as under different oscillation conditions using a Student's t-test. $p < 0.05$ was considered to indicate statistically significant differences.

RESULTS AND DISCUSSION

1. Comparison of the Q Factors of the Q-sense and VNA-based QCM. The quality factor of the crystal needs to be established from the ratio of the resonance frequency and the damping, as measured by "ring-down" experiments for the Q-sense and impedance analysis for the VNA-based QCM. Table 2 summarizes the Q factors for both QCM instruments. Q factors for both instruments show no significant differences (Student's t-test $p < 0.05$), neither between instruments nor between hydrophilic and hydrophobic crystals and increase with overtone number from around 3000 to 12000. The Q factors in Table 2 are relatively low as they pertain to oscillations in a liquid phase, whereas in air Q factors ranging from 55000 to 100000 have been calculated.[7,12] The larger Q factor values in air are due to slower dampening of oscillations in air than in an aqueous phase (see also Figure 4).

Table 2 Quality factors, Q for the Q-sense and VNA-based QCM for hydrophilic and hydrophobic SAM-coated crystals at six different overtones. Data represent averages ± standard deviations over triplicate experiments with separate crystals.

	VNA-based		**Q-sense**	
Overtone (n)	**Hydrophobic** crystal	**Hydrophilic** crystal	**Hydrophobic** crystal	**Hydrophilic** crystal
1	3266 ± 74	3368 ± 122	3364 ± 23	3057 ± 577
3	5754 ± 96	5901 ± 114	5992 ± 31	5884 ± 159
5	7216 ± 560	7621 ± 150	7359 ± 46	7307 ± 43
7	8956 ± 122	9133 ± 107	8477 ± 68	8466 ± 207
9	10105 ± 141	10358 ± 66	10265 ± 133	10272 ± 351
11	11451 ± 172	11615 ± 575	11519 ± 215	11602 ± 410

Combination of the Q factors with the driving voltage, allows to calculate the oscillation forces on adsorbed masses or adhering (bio)colloidal particles according to Eqs. 7 and 8, respectively, provided the driving voltage is known which is not the case for the Q-sense. In this study, we will adapt the Q factor measured for the third overtone (15 MHz) for the calculation of oscillation forces. Use of the third overtone is common in QCM analyses, as it prevails in the center of the crystal, while higher overtones become more prominent toward the edges of the crystal.[2] Resulting oscillation forces for our VNA-based QCM are compared in Table 3 with oscillation forces obtained in other studies, together with the resonance frequencies, Q factors, particle radii and driving voltages applied. The data compiled in Table 3 in essence represent the proportionality of $F_{osc\text{-}P}$ on f_0^2, R^2 and Q^2, and importantly demonstrate that the characteristics obtained for our VNA-based QCM are in line with available literature data.

Table 3 Comparison of resonance frequencies, Q factors, particle radii and driving voltages together with the resulting oscillation forces on a spherical particle (radius (R)) adhering on an oscillating crystal surface in an aqueous phase, as obtained in this study and reported in the literature.

Reference	f_0	Q	R	F_{osc-P} (pN)					
				0.01	0.1	0.4	3.5	6	10
	(MHz)		(μm)	(V)	(V)	(V)	(V)	(V)	(V)
This study	5	5900*	0.5	0.2	2	30	-	-	-
Edvardsson et al[21]	5	2500	0.1	-	-	-	-	-	16
Yuan et al[6]	10	4000	3	-	-	-	17900	-	
Dultsev et al[4]	15	5000	2.5	-	-	-	-	129200	-

*average Q factor obtained for hydrophilic and hydrophobic crystals obtained from the third overtone.

2. Detachment forces of adhering (bio)colloidal particles. In a first series of experiments, streptococci and polystyrene particles were allowed to adhere during 1 h from a flowing suspension to hydrophobic and hydrophilic crystal surfaces in absence and presence of crystal oscillation, followed by 30 min application of an oscillation force to stimulate particle detachment. Both streptococci and polystyrene particles adhered in numbers in the order of 10^{10} m^{-2} (Table 4), corresponding with a surface coverage of around 1-10%, low enough to prevent direct interactions between adhering particles during crystal oscillation.

Table 4 Number of streptococci and polystyrene particles adhering after 1 h from a flowing suspension to hydrophilic and hydrophobic crystal surfaces in absence and presence of crystal's oscillations, followed by 30 min application of three different oscillation forces. Data represents averages with standard deviations over two separate experiments.

During adhesion	N_p after adhesion ($x10^{10}$ m^{-2})		During detachment	N_p after detachment ($x10^{10}$ m^{-2})	
F_{osc-P} (pN)	Hydrophilic crystal	Hydrophobic crystal	F_{osc-P} (pN)	Hydrophilic crystal	Hydrophobic crystal
***S. salivarius* HB7**					
0	6.1 ± 0.4	4.6 ± 0.6	0.2	6.1 ± 0.4	4.6 ± 0.6
0			2	6.3 ± 0.8	5.6 ± 1.0
0			30	5.9 ± 0.5	4.0 ± 0.4
2	4.7 ± 0.3	4.8 ± 0.3	30	4.7 ± 0.7	4.8 ± 0.1
***S. salivarius* HBC12**					
0	2.1 ± 0.1	2.9 ± 0.7	0.2	2.2 ± 0.2	2.8 ± 0.7
0			2	1.7 ± 0.7	2.5 ± 0.8
0			30	1.5± 0.1	2.1 ± 0.6
2	2.0 ± 0.0	1.6 ± 0.2	30	1.6 ± 0.1	1.6 ± 0.2
Polystyrene particles					
0	3.5 ± 0.7	3.9 ± 1.1	0.2	3.9 ± 0.6	3.7 ± 0.0
0			2	2.9 ± 0.4	3.2 ± 0.3
0			30	0.2 ± 0.0	0.4 ± 0.1
2	3.5 ± 0.1	1.7 ± 0.3	30	0.9 ± 0.2	0.6 ± 0.0

S. salivarius HB7, being relatively hydrophobic compared to *S. salivarius* HBC12 and possessing 91 nm long fibrillar surface tethers, adhered in higher numbers to the hydrophilic crystal as compared with the hydrophobic crystal in absence of crystal oscillation. However, upon application of a minor oscillation force during adhesion the number of adhering *S. salivarius* HB7 reduced on the hydrophilic crystal to become equal on both crystals. Subsequent application of a higher oscillation force did not cause significant detachment of adhering streptococci. For *S. salivarius* HBC12, possessing no demonstrable fibrillar surface tethers, no significant differences in numbers of adhering bacteria were found on both crystals, nor did application of an oscillation force during adhesion affect adhesion.

However, during the detachment phase of the experiment, streptococci that had adhered in absence of crystal oscillations, detached with increasing oscillation forces.

The lower adhesion numbers of *S. salivarius* HBC12, being more hydrophilic and without demonstrable fibrillar surface tethers as compared with *S. salivarius* HB7, has been described as a result of the greater thermodynamic preference of *S. salivarius* HB7 to adhere to surfaces from an aqueous phase, possessing an interfacial free energy of adhesion that is across the different crystal surfaces around 13 mJ m^{-2} more negative for *S. salivarius* HB7 than for HBC12. Also, its possession of fibrillar surface tethers allows *S. salivarius* HB7 to spring-couple itself through its tethers directly to a substratum surface, therewith overcoming the potential energy barrier between negatively charged substratum surfaces and its own negative charge. Clearly, this yields a strong bond that cannot be disrupted by the oscillation forces applied. *S. salivarius* HBC12 on the other hand, has been described to adhere in a "floating" mode within the secondary interaction minimum at variable distance above the substratum surface and the oscillation forces applied after adhesion were sufficient to push the organism out of the secondary energy minimum and cause detachment (see also Table 4). Adhesion under higher oscillation forces may have selected for strongly adhering bacteria from a suspension, as in those cases application of a higher oscillation force did not yield significant bacterial detachment for neither strain.

The polystyrene particles employed in this study are based on a comparison of polystyrene and *S. salivarius* water contact angles, more hydrophobic[22] than the bacterial strains, allowing them to more closely approach to substratum surfaces. In absence of oscillation, they adhere in similar numbers to the hydrophilic and hydrophobic crystals alike *S. salivarius* HB7, but in presence of an oscillation force, adhesion to the hydrophobic crystal is significantly reduced. Different than its bacterial counterpart, the inert colloidal particle does not possess long surface tethers to spring-couple itself to the substratum and significant detachment can be induced by crystal oscillations applied after the adhesion phase.

3. Forces Required to Prevent Adhesion. (Bio)colloidal particle adhesion was also carried out to an oscillating crystal during oscillations at different oscillation forces without being followed by a detachment phase in order to determine the oscillation force preventing adhesion. Oscillation during adhesion, did not impede spring-coupled adhesion of *S. salivarius* HB7 to hydrophobic crystals, but a minor decrease in adhesion was observed on hydrophilic crystal surfaces compared to absence of oscillation during adhesion (Table 5). The more hydrophilic *S. salivarius* HBC12 showed a strong reduction in adhesion during crystal oscillation at an oscillation force of 30 pN. Similarly, polystyrene particles were greatly discouraged to adhere when the oscillation force during adhesion was 30 pN, especially from the hydrophilic crystal. These observations suggest that rotation and wiggling of

adhering *S. salivarius* HB7 may lead to an increase of the number of tethers involved in the coupling, resulting in stronger adhesion than can be achieved for (bio)colloidal particles lacking surface tethers.[11]

Comparison of the bacterial adhesion forces obtained from literature is difficult, because a clear distinction between forces to prevent adhesion and forces to detach adhering bacteria is not always trivial in the literature. Moreover, bacterial adhesion forces reported can vary by orders of magnitude depending on the method applied. Atomic force microscopy (AFM) has so far yielded the largest adhesion forces in the literature ranging up to 50000 pN,[23] roughly 1500 – 2000 times larger than applied using the oscillating crystal method here. This might be caused amongst others, by the fact that in AFM bacteria are forced into contact with a substratum surface under an applied loading force, after which detachment is initiated and an adhesion force ("detachment") is measured. However, using optical tweezers that also require a forced albeit possibly more gentle, contact, adhesion forces in a detachment mode for coccal bacteria of around 20 pN were obtained,[24] resembling the values obtained in this study. Flow displacement systems allow to make a clear distinction between forces to prevent adhesion to forces to cause detachment and fluid shear forces of around 20 pN[10] were found sufficient to prevent adhesion of coccal bacteria, while bacterial detachment required a fluid shear forces up to 42 pN.[10] This comparison puts data obtained with optical tweezers, flow displacement systems and QCM at equal values, making AFM adhesion data unrealistically high. Also, it partly negates frequently voiced criticism on QCM data that the adhesion process may be influenced by the high frequencies at which the substratum oscillates during adhesion. However, the influence of substratum oscillations upon the adhesion process is dependent on whether bacteria adhere in a "spring-coupled" or "floating mode" like *S. salivarius* HB7 and HBC12 respectively and caution thus remains necessary when interpreting QCM data.

Forces to prevent bacterial adhesion arising from flow displacement data, are obtained using a uni-directional force upon the bacteria, while in QCM the crystal oscillates and accordingly the direction of the forces changes at high frequency. Whereas this does not clearly show from major differences in adhesion force values obtained in flow displacement systems, the spatial distribution of adhering bacteria is affected (Figure 5). Both strains of streptococci as well as polystyrene particle adhere homogeneously distributed and mainly as single particles during adhesion in absence of crystal oscillation, like they do under flow. Adhesion on oscillating crystals shows surface aggregation of *S. salivarius* HB7 and polystyrene particles, which is most predominant for *S. salivarius* HB7. This implies that in absence of oscillation, streptococci may remain longer in their so-called "mobile" adhesion phase, while they may tumble over their comb of fibrillar surface tethers till they become immobilized in a surface aggregate during presence of oscillation. Note, that the microscopic images obtained of adhering bacteria on oscillating crystals have been taken from the center of the crystal, where

oscillation amplitudes are maximal.[21] Calculation of the distribution of adhering bacteria over the crystal surface would therefore be interesting to pursue.

Table 5 The number of streptococci and polystyrene particles after adhesion during application of different oscillation forces F_{osc-P} to a hydrophilic and hydrophobic crystal surface. Data represents averages with standard deviations over two separate experiments.

During adhesion	**N_p after adhesion ($x10^{10}$ m^{-2})**	
F_{osc-P} (pN)	**Hydrophilic crystal**	**Hydrophobic crystal**
***S. salivarius* HB7**		
0	6.1 ± 0.4	4.6 ± 0.6
0.2	4.8 ± 0.0	4.1 ± 0.1
2	4.8 ± 0.2	4.9 ± 0.2
30	4.2 ± 2.1	5.0 ± 0.9
***S. salivarius* HBC12**		
0	2.9 ± 0.1	2.9 ± 0.7
0.2	2.1 ± 0.4	2.4 ± 0.1
2	2.0 ± 0.1	1.6 ± 0.1
30	0.6 ± 0.2	1.5 ± 0.5
Polystyrene particles		
0	3.5 ± 0.7	3.9 ± 1.1
0.2	4.1 ± 0.5	3.6 ± 0.2
2	4.1 ± 0.2	1.8 ± 0.2
30	0.2 ± 0.0	1.5 ± 0.8

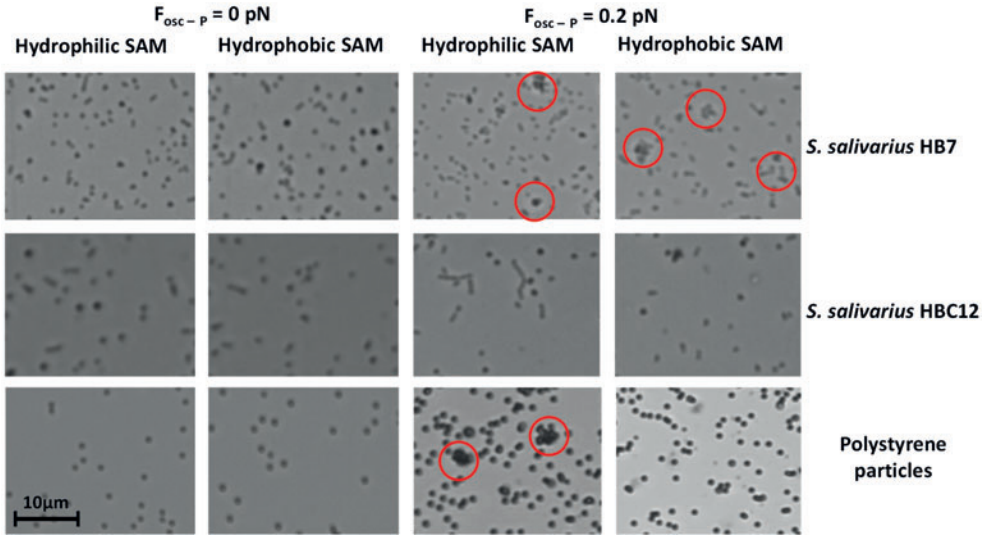

Figure 5. Distribution of adhering *S. salivarius* HB7, *S. salivarius* HBC12 and polystyrene particles to hydrophilic and hydrophobic crystals after adhesion in absence and presence of oscillation forces (F_{osc-P} = 0.2 pN). Scale bar corresponds to 10 µm, while surface aggregation of particles is indicated by red circles.

4. Kelvin-Voigt Analyses of QCM Data. In order to see whether the spring constants and drag coefficients of the bond with the crystal surface, including particle masses derived, depend on the oscillation forces applied during adhesion, adhesion was allowed in absence and presence of crystal oscillations followed by QCM measurements and fitting of the data to a phenomenological Kelvin-Voigt model (see Figures 6 and 7 for results on a hydrophobic and hydrophilic crystal, respectively). As can be seen the quality of the fit is rather good (see also Table 6), while within the window of observable resonance frequencies positive frequency shifts or frequencies of zero crossing are observed, except for S. *salivarius* HBC12 on the hydrophobic crystal, confirming its known tendency to mass couple to a substratum surface.[25]

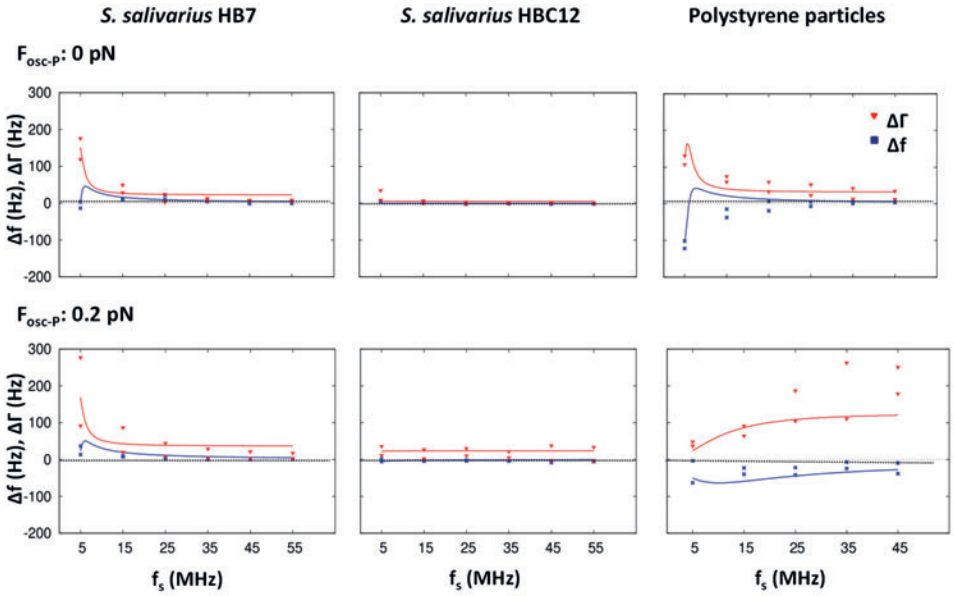

Figure 6. QCM responses, Δf and ΔΓ as a function of the crystal oscillation frequency for adhesion of *S. salivarius* HB7, *S. salivarius* HBC12 and polystyrene particles on hydrophobic crystals after 1 h adhesion in absence (top panels) and presence of crystal oscillation (0.2 pN; bottom panels), followed by 30 min oscillation and measurement at the same oscillation force. Data represent duplicate experiments.

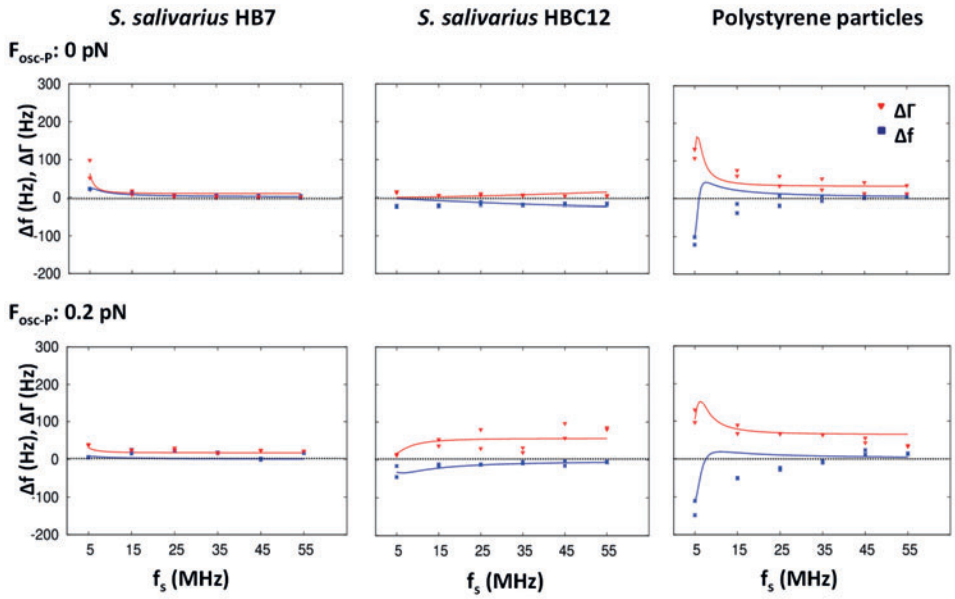

Figure 7. QCM responses, Δf and ΔΓ as a function of the crystal oscillation frequency for adhesion of *S. salivarius* HB7, *S. salivarius* HBC12 and polystyrene particles on hydrophilic crystals after 1 h adhesion in absence (top panels) and presence of crystal oscillation (0.2 pN; bottom panels), followed by 30 min oscillation and measurement at the same oscillation force. Data represent duplicate experiments.

Table 6 summarizes the resulting bond parameters fitted to the VNA-based QCM output. For *S. salivarius* HB7, adhesion in absence of oscillations yields lower particle masses, slightly higher spring constants and drag coefficients than obtained when adhesion occurs under an oscillation force of 0.2 pN and regardless of the hydrophobicity of the crystal surface. Also for *S. salivarius* HBC12 and polystyrene particles, it can be seen that adhesion in absence of oscillations yields lower particle masses, despite the 30 min application of an oscillation force of 0.2 pN to detach adhering particles. However, for the particles still adhering when QCM measurements starts, this 30 min time period may also act as a bond maturation time period during which the number of binding tethers may increase and aggregates are formed (see Figure 5). As a simple explanation for the increases in particle masses observed for *S. salivarius* HB7 and polystyrene particles, it is suggested that this is due to aggregate formation as the increase ratio roughly matches the number of particles that can be discerned in the aggregates. Aggregate formation also increases the total number of tethers, i.e. binding tethers in the entire aggregate coupled to the surface, explaining the increase in spring constant observed. Along the same lines, but now with respect to volume, aggregate formation may explain why the drag coefficients measured are larger in case of adhesion under and applied oscillation force. This explanation does not hold however for more hydrophilic *S. salivarius* HBC12. The drag coefficient for

S. salivarius HBC12 on hydrophilic crystal is much higher compared to on the hydrophobic crystal, possibly due to differential structuring of water. On the hydrophilic crystal, the ratio between electron-donating and accepting surface free energy parameters is large (Table 1) indicating that in order to contact the crystal surface the bacterium has to permeate a highly structured water layer.[26] This may lead to a larger drag coefficient. This explanation evidently cannot be extrapolated to bacteria with surface tethers on their outermost surface, because they keep a larger distance from the surface.

Table 6 Spring constants k, drag coefficients ξ, masses m_p, and RMSD values obtained in the Kelvin-Voigt coupled-resonator model, for *S. salivarius* HB7 with fibrillar surface tethers, bald *S. salivarius* HBC12 and abiotic polystyrene particles on hydrophilic SAM-coated crystals and hydrophobic SAM-coated crystals.

F_{osc-P}(pN)			m_p (x 10^{-16} Kg)		k (kg s^{-2})		ξ (x10^{-9} Kg s^{-1})		RMSD (Hz)	
During adhesion	During detachment	During measurement	Hydro phobic	Hydro philic	Hydro phobic	Hydro philic	Hydro phobic	Hydro philic	Hydro phobic	Hydro philic
***S. salivarius* HB7**										
0	0.2	0.2	2.7	1.0	0.2	0.1	3.0	1.0	14.5*	11.0*
0.2	0.2	0.2	4.2	4.3	0.8	0.2	26.9	5.0	69.4*	13.0*
***S. salivarius* HBC12**										
0	0.2	0.2	0.0	0.3	1.0	0.0	0.0	17.0	0.0	9.9
0.2	0.2	0.2	4.7	2.6	0.0	0.3	3.0	15.0	10.9*	18.7*
Polystyrene particles										
0	0.2	0.2	3.3	3.8	0.4	0.5	5.0	9.0	22.4*	28.6*
0.2	0.2	0.2	5.8	4.8	0.0	0.0	36.9	22.9	76.5*	42.4*

*Positive frequency shifts or frequencies of zero crossing observed within the window of observable resonance frequencies.

CONCLUSION

In summary, the study performed here offers a new, and versatile as well as low cost quantitative tool for the determination of forces involved in (bio)colloidal particle adhesion. Adhesion force values obtained using the QCM crystal as an oscillating substratum, coincide well with data obtained using optical tweezers and flow displacement systems. Despite the lack of influence of substratum oscillation upon the adhesion forces measured, the characteristics of the bond as obtained in a coupled-resonator, Kelvin-Voigt based model are dependent on the development history of the bond, i.e. on the oscillation forces felt by (bio)colloidal particles during adhesion.

ACKNOWLEDGEMENTS

The authors like to thank Prof. Diethelm Johannsmann, Clausthal University of Technology, Germany for providing the software package QTZ, that turns the basic VNA into a QCM. The authors declare no potential conflicts of interest with respect to authorship and/or publication of this article. HJB is also director of a consulting company SASA BV. Opinions and assertions contained herein are those of the authors and are not construed as necessarily representing views of the funding organization or their respective employer(s).

REFERENCES

(1) Sauerbrey, G. Verwendung von Schwingquarzen Zur Wägung Dünner Schichten Und Zur Mikrowägung. *Zeitschrift für Physik*. **1959**, *155,* 206–222.

(2) Edvardsson, M.; Rodahl, M.; Kasemo, B.; Höök, F. A Dual-Frequency QCM-D Setup Operating at Elevated Oscillation Amplitudes. *Anal. Chem.* **2005**, *77*, 4918–4926.

(3) Pomorska, A.; Shchukin, D.; Hammond, R.; Cooper, M. A.; Grundmeier, G.; Johannsmann, D. Positive Frequency Shifts Observed upon Adsorbing Micron-Sized Solid Objects to a Quartz Crystal Microbalance from the Liquid Phase. *Anal. Chem.* **2010**, *82*, 2237–2242.

(4) Dultsev, F. N.; Ostanin, V. P.; Klenerman, D. "Hearing" Bond Breakage. Measurement of Bond Rupture Forces Using a Quartz Crystal Microbalance. *Langmuir* **2000**, *16*, 5036–5040.

(5) Van Der Werff, M. J.; Yuan, Y. J.; Hirst, E. R.; Xu, W. L.; Chen, H.; Bronlund, J. E. Quartz Crystal Microbalance Induced Bond Rupture Sensing for Medical Diagnostics. *IEEE Sens. J.* **2007**, *7*, 762–769.

(6) Yuan, Y. J.; Jia, R. Study on Pivot-Point Vibration of Molecular Bond-Rupture Events by Quartz Crystal Microbalance for Biomedical Diagnostics. *Int. J. Nanomedicine* **2012**, *7*, 381–391.

(7) Borovsky, B.; Mason, B. L.; Krim, J. Scanning Tunneling Microscope Measurements of the Amplitude of Vibration of a Quartz Crystal Oscillator. *J. Appl. Phys.* **2000**, *88*, 4017.

(8) Dufrene, Y. F. Atomic Force Microscopy , a Powerful Tool in Microbiology. *J. Bacteriol.* **2002**, *184*, 5205–5213.

(9) Simpson, K. H.; Bowden, G.; Höök, M.; Anvari, B. Measurement of Adhesive Forces between Individual *Staphylococcus Aureus* MSCRAMMs and Protein-Coated Surfaces by Use of Optical Tweezers. *J. Bacteriol.* **2003**, *185*, 2031–2035.

(10) Boks, N. P.; Norde, W.; Van der Mei, H. C.; Busscher, H. J. Forces Involved in Bacterial Adhesion to Hydrophilic and Hydrophobic Surfaces. *Microbiology* **2008**, *154*, 3122–3133.

(11) Sjollema, J.; Van der Mei, H. C.; Hall, C. L.; Peterson, B. W.; De Vries, J.; Song, L.; De Jong, E. D.; Busscher, H. J.; Swartjes, J. J. T. M. Detachment and Successive Re-Attachment of Multiple, Reversibly-Binding Tethers Result in Irreversible Bacterial Adhesion to Surfaces. *Sci. Rep.* **2017**, *7*, 4369.

(12) Kanazawa, K. K. Mechanical Behaviour of Đlms on the Quartz Microbalance. *Faraday Discuss* **1997**, *107*, 77–90.

(13) Van der Westen, R.; Sharma, P. K.; De Raedt, H.; Vermue, I.; Van der Mei, H. C.; Busscher, H. J. Elastic and Viscous Bond Components in the Adhesion of Colloidal Particles and Fibrillated Streptococci to QCM-D Crystal Surfaces with Different Hydrophobicities Using Kelvin–Voigt and Maxwell Models. *Phys. Chem. Chem. Phys.* **2017**, *19*, 25391–25400.

(14) D'Amour, J. N.; Stålgren, J. J. R.; Kanazawa, K. K.; Frank, C. W.; Rodahl, M.; Johannsmann, D. Capillary Aging of the Contacts between Glass Spheres and a Quartz Resonator Surface. *Phys. Rev. Lett.* **2006**, *96,* 058301.

(15) Johannsmann, D. Introduction. In *The Quartz Crystal Microbalance in Soft Matter Research: Fundamentals and Modeling*; Johannsmann, D., Ed.; Springer International Publishing, **2015**, 1–22.

(16) Beck, R.; Pittermann, U.; Weil, K. G. Impedance Analysis of Quartz Oscillators, Contacted on One Side with a Liquid. *Berichte der Bunsengesellschaft für Phys. Chemie* **1988**, *92*, 1363–1368.

(17) Reviakine, I.; Johannsmann, D.; Richter, R. P. Hearing What You Cannot See and Visualizing What You Hear. *Anal. Chem.* **2011**, *83*, 8838–8848.

(18) Van der Mei, H. C.; Leonard, A. J.; Weerkamp, A. H.; Rouxhet, P. G.; Busscher, H. J. Surface Properties of *Streptococcus salivarius* HB and Nonfibrillar Mutants: Measurement of Zeta Potential and Elemental Composition with X-Ray Photoelectron Spectroscopy. *J. Bacteriol.* **1988**, *170*, 2462–2466.

(19) Peschel, A.; Langhoff, A.; Johannsmann, D. Coupled Resonances Allow Studying the Aging of Adhesive Contacts between a QCM Surface and Single, Micrometer-Sized Particles. *Nanotechnology.* **2015**, *26*, 484001.

(20) Olsson, A. L. J.; Van der Mei, H. C.; Johannsmann, D.; Busscher, H. J.; Sharma, P. K. Probing Colloid-Substratum Contact Stiffness by Acoustic Sensing in a Liquid Phase. *Anal. Chem.* **2012**, *84*, 4504–4512.

(21) Edvardsson, M.; Rodahl, M.; Höök, F. Investigation of Binding Event Perturbations Caused by Elevated QCM-D Oscillation Amplitude. *Analyst* **2006**, *131*, 822–828.

(22) Zhang, L.; Torkelson, J. M. Enhancement of Surface Wettability by Incorporating Polar Initiator Fragments at Chain Ends of Low-Molecular-Weight Polymers. *ACS Appl. Mater. Interfaces* **2017**, *9*, 12176–12181.

(23) Bowen, W. R.; Fenton, A. S.; Lovitt, R. W.; Wright, C. J. The Measurement of *Bacillus mycoides* Spore Adhesion Using Atomic Force Microscopy, Simple Counting Methods, and a Spinning Disk Technique. *Biotechnol. Bioeng.* **2002**, *79*, 170–179.

(24) Simpson, K. H.; Bowden, M. G.; Höök, M.; Anvari, B. Measurement of Adhesive Forces between *S. epidermidis* and Fibronectin-Coated Surfaces Using Optical Tweezers. *Lasers Surg. Med.* **2002**, *31*, 45–52.

(25) Olsson, A. L. J.; Van der Mei, H. C.; Busscher, H. J.; Sharma, P. K. Influence of Cell Surface Appendages on the Bacterium-Substratum Interface Measured Real-Time Using QCM-D. *Langmuir* **2009**, *25*, 1627–1632.

(26) Van Oss, C. J.; Giese, R. F. Role of the Properties and Structure of Liquid Water in Colloidal and Interfacial Systems. *J. Dispers. Sci. Technol.* **2004**, *25*, 631–655.